JACS
JOURNAL OF THE AMERICAN CHEMICAL SOCIETY
Communication
pubs.acs.org/JACS

Encapsulation of Xenon by a Self-Assembled Fe_4L_6 Metallosupramolecular Cage

Juho Roukala,[†] Jianfeng Zhu,[†,‡] Chandan Giri,[§] Kari Rissanen,[§] Perttu Lantto,*[,†] and Ville-Veikko Telkki*[,†]

[†]NMR Research Group, Centre for Molecular Materials, University of Oulu, 90014 Oulu, Finland
[‡]Department of Chemistry, University of Sheffield, Sheffield S3 7HF, United Kingdom
[§]Department of Chemistry, Nanoscience Center, University of Jyväskylä, 40014 Jyväskylä, Finland

Supporting Information

ABSTRACT: We report ^{129}Xe NMR experiments showing that a Fe_4L_6 metallosupramolecular cage can encapsulate xenon in water with a binding constant of 16 M^{-1}. The observations pave the way for exploiting metallosupramolecular cages as economical means to extract rare gases as well as ^{129}Xe NMR-based bio-, pH, and temperature sensors. Xe in the Fe_4L_6 cage has an unusual chemical shift downfield from free Xe in water. The exchange rate between the encapsulated and free Xe was determined to be about 10 Hz, potentially allowing signal amplification via chemical exchange saturation transfer. Computational treatment showed that dynamical effects of Xe motion as well as relativistic effects have significant contributions to the chemical shift of Xe in the cage and enabled the replication of the observed linear temperature dependence of the shift.

The understanding of the self-assembly properties, structures, and functionalities of metallosupramolecular cage structures is one of the major challenges of supramolecular chemistry. The most recent area in metallosupramolecular chemistry[1] is the utilization of subcomponent self-assembly, in which structures are generated *in situ* from their, often simple, subcomponents.[2] This growing line of research enables the construction of complex 3D structures[3] through spontaneous and hierarchical assembly utilizing chemical reactions and reversible noncovalent intermolecular interactions. When metal ions are essential components of the self-assembly, the molecular architecture of these self-assembled 3D objects heavily depends on the coordination geometry of the metal ion used.[2b]

The metal ion-assisted subcomponent self-assembly of an aromatic linear rigid bis-amine, 2-formylpyridine and Fe(II) ions resulting in a tetrahedral $\mathbf{M_4L_6}$ cage in aqueous media reported jointly by Nitschke and Rissanen opened a new route to molecular tetrahedral complexes.[4] Later, the host–guest chemistry of the same tetrahedral cage was explored, demonstrating its potential as a container molecule for white phosphorus.[5] Recently, we have expanded the same methodology to Co(II) and Ni(II) ions resulting in analogous tetrahedral $\mathbf{M_4L_6}$ cage complexes with similar host–guest properties.[6] Selecting very small subcomponents and using the same methodology it was possible to construct the smallest possible tetrahedral $\mathbf{M_4L_6}$ cage.[7]

Xenon (Xe) is a noble gas occurring naturally in the atmosphere at 0.087 ppm by volume (ppmv). The nuclear magnetic resonance (NMR) sensitivity of ^{129}Xe (spin-1/2 nucleus) can be increased by 4–5 orders of magnitude by spin exchange optical pumping (SEOP) hyperpolarization method, and due to the large, polarizable electron cloud, the chemical shift of ^{129}Xe is extremely sensitive to its local environment.[8] Consequently, Xe has been widely used as an inert probe, e.g., in magnetic resonance imaging (MRI) of lungs,[9] microfluidic flow imaging,[10] investigation of liquid crystals,[11] and polymers[12] as well as determination of pore sizes of porous media.[13] The strong, linear temperature dependence of the chemical shift of ^{129}Xe dissolved in a liquid (typical slope about −0.4 ppm/K) has also been exploited for accurate NMR monitoring of sample temperature.[14] A recent, very exciting application of ^{129}Xe NMR is so-called xenon biosensor, in which Xe is trapped in cryptophane cages functionalized to bind to a specific analyte.[15] The binding is observed through the changes in the ^{129}Xe chemical shift, and the spatial distribution of the binding sites is determined through MRI data.[16] Cryptophane encapsulated Xe can also be used as temperature sensor due to the linear temperature dependence of its chemical shift (slope from 0.08 to 0.3 ppm/K)[17] and even local pH sensors.[18]

It is uncommon for metallosupramolecular cages to bind gases in solution, and a preliminary observation reports that Fe_4L_6 cages have no affinity for Xe.[19] Herein, we describe ^{129}Xe NMR experiments and computational modeling that unambiguously show (contrary to ref 19) the encapsulation of Xe by Fe_4L_6 in water, demonstrating the potential of metallosupramolecular cages, e.g., as more economical means to extract rare gases as compared to cryogenic methods[20] and alternative, low cost cages in the above-mentioned ^{129}Xe NMR applications.

The anionic iron(II) tetrahedral $[Fe_4L_6]^{4-}$ cage **1** (Figure 1a) was synthesized in D_2O through subcomponent self-assembly as described elsewhere.[4] The metal centers are located at the vertices of the tetrahedron, and the ligands bridging them form the six edges. The 12 sulfonate groups (two on each ligand), located on the exterior of the cage, provide good water

Received: December 22, 2014
Published: February 5, 2015

DOI: 10.1021/ja5130176
J. Am. Chem. Soc. 2015, 137, 2464–2467

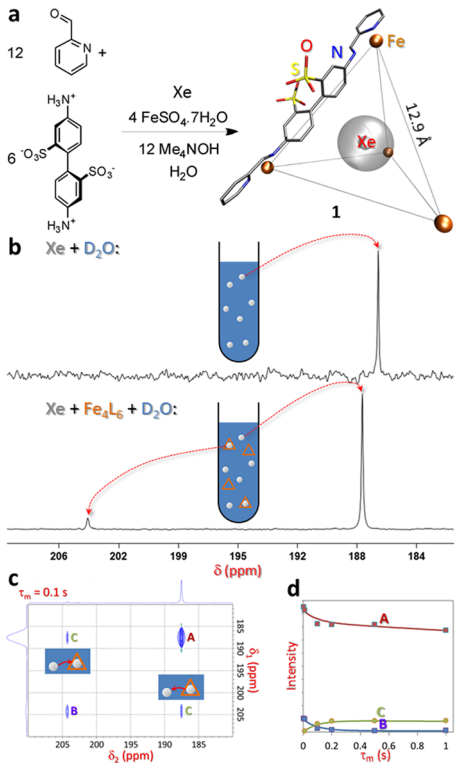

Figure 1. (a) The synthesis of the Fe_4L_6 cage **1** with a Xe atom in its cavity. Only one of tetrahedron edges is shown for clarity. (b) ^{129}Xe NMR spectra of Xe in D_2O (top) and in **1**/D_2O solution (bottom) measured at 298 K. (c) 2D ^{129}Xe EXSY spectrum measured with mixing time τ_m of 100 ms at 298 K. (d) Intensities of the EXSY peaks as a function of mixing time. Solid lines represent the two-site exchange model fit.[25]

solubility (34 g/L), while the aromatic rings provide a hydrophobic interior and thus the encapsulation of several guests due to hydrophobic effects.[4] The average Fe−Fe separation is 12.9 Å, and the cage possesses a volume of 141 Å^3,[4] suggesting that Xe atom (van der Waals diameter 4.32 Å, corresponding volume 42.2 Å^3) fits well in the cage.

After the synthesis, about 4.9 bar Xe gas atmosphere was added to the sample tube. ^{129}Xe NMR spectrum (Figure 1b, see experimental details in Supporting Information (SI)) shows the encapsulation of Xe in **1**/D_2O solution due to the hydrophobic effects.[4,5] The spectrum includes two signals at 187.7 and 204.3 ppm (with respect to the chemical shift of Xe gas), the former arising from Xe dissolved in D_2O (see the comparison with the ^{129}Xe spectrum of Xe in pure D_2O in Figure 1b) and the latter from the encapsulated Xe. We note that the latter signal cannot arise from an interaction between Xe and some subcomponent (or exterior of the cage), because such an interaction should result in an unrealistically long-living Xe-subcomponent pair to be observed as a separate, sharp NMR signal. Considering the molarity of the cage (8.9 mM) and the Xe solubility (20 mM)[21] in H_2O at 298 K and 4.9 bar, an intensity ratio of 1.0:9.1 of the two signals suggests only 24% of the cages contain Xe atoms (assuming that one cage can encapsulate only one Xe, as a single cage signal implies). The amount of dissolved and encapsulated Xe could be increased by bubbling Xe through the solution.[22] Xe binding constant for **1** estimated through the intensities of the peaks in the ^{129}Xe spectrum is about 16 M^{-1}, which is much lower than in the case of SF_6 (1.3×10^4 M^{-1}),[19] likely due to the less optimal ratio of the volume of the atom to the volume enclosed by the cage (30% for Xe vs 53% for SF_6). Xe@**1** resonates at 16.6 ppm higher chemical shift than free Xe in D_2O, whereas usually in the cryptophane cages the shift is lower.[16] Fairchild et al.[23] have also reported a high chemical shift of ^{129}Xe in cryptophane functionalized with six cationic [Cp*Ru] moieties, highlighting both electron-withdrawing and relativistic effects of the metals on the chemical shift, later explained in detail by first-principles modeling.[24]

Appearance of cross peaks (signals C in Figure 1c) in 2D ^{129}Xe exchange spectroscopy (EXSY)[25] spectrum at the mixing time of 100 ms reveals that the Xe in **1** undergoes chemical exchange with the Xe in D_2O. Least-squares fits of two site exchange model[25] to the intensities of the diagonal and cross peaks measured as a function of the mixing time yielded the rate constant of 10 Hz. Consequently, the exchange is slow in the NMR time-scale (resulting in separated, narrow signals from each site)[26] and fast in the relaxation time-scale (according to the fit, T_1 relaxation time in the cage is about 11 s and much longer in the solution), which provides the opportunity to boost significantly the sensitivity by means of chemical exchange saturation transfer of hyperpolarized xenon (HYPER-CEST)[15b] approach in potential ^{129}Xe NMR applications. The molar fractions of Xe in the cage and solvent resulting from the fit are 9.4% and 91.6%, respectively, being consistent with the peak intensities obtained by integrating the signals in Figure 1b. The observed exchange rate is an additional proof that that the downfield signal really arises from Xe inside the cage; an interaction with a subcomponent or exterior of the cage cannot result in such a slow exchange rate.

^{129}Xe NMR spectra measured at variable temperature (Figure 2a) provide additional insight into the dynamics of the system. Typically, the chemical shift of ^{129}Xe dissolved in a liquid decreases linearly with increasing temperature due to the linear decrease of the liquid density,[27] but the chemical shift of Xe dissolved in D_2O shows a surprising, nonlinear behavior, first increasing with increasing temperature, reaching a maximum

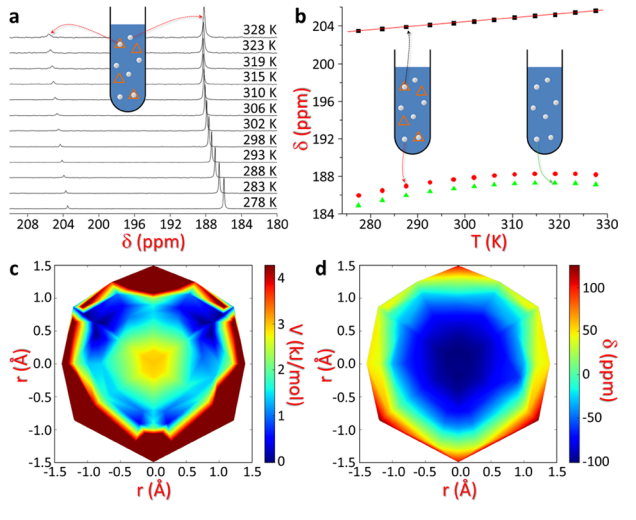

Figure 2. (a) ^{129}Xe NMR spectra as a function of temperature of Xe in **1**/D_2O solution. (b) ^{129}Xe chemical shifts as a function of temperature of Xe in **1**/D_2O solution (black square: cage signal; red circle: solution signal) and in D_2O (green triangle). Red line represents the linear fit to the cage signal data points. Calculated (c) potential energy and (d) chemical shift surfaces of Xe in the cage in a plane defined by the geometric center (at $r = 0$) and two corners (symmetrically upward) of the cage.

DOI: 10.1021/ja5130176
J. Am. Chem. Soc. 2015, 137, 2464−2467

value at 319.0 K (46.0 °C) and then decreasing with further increasing of the temperature (Figure 2b). Exactly the same trend was observed for the sample of Xe in pure D_2O (Figure 2b). This unusual behavior will be analyzed and explained in detail in a separate study. In contrast, the chemical shift of ^{129}Xe in cage **1** increases linearly with increasing temperature, like in the case of cryptophane cages.[17b] The slope and *y* intercept of the line fitted to the data points (Figure 2b) are (0.0422 ± 0.0006) ppm/K and (191.8 ± 0.2) ppm, respectively. The slope is smaller than in the case of Xe in cryptophanes, where it varies from 0.08 to 0.3 ppm/K.[17b] The line widths of both the solution and cage signals increase with increasing temperature, indicating significantly faster chemical exchange at higher temperatures. ^{1}H NMR spectra (Figure S1) indicate that the expansion of Fe_4L_6 cage is smaller due to encapsulation of Xe than cyclohexane and the cages are expanding more at higher temperatures.

Quantum chemical density functional theory (DFT) calculations of potential energy and NMR shielding of Xe were performed with a fixed-geometry Fe_4L_6 cage,[6] without solvent, using Turbomole[28] and Dalton[29] codes. We used all-electron co-r/def2-SVP[30] basis sets (Table S2) for the Xe/cage atoms and BHandHLYP[31] functional benchmarked against ab initio calculations in earlier studies of Xe chemical shift,[32,33] yielding the smallest, i.e., least overestimated Xe chemical shift of the tested functionals (see Table S3 in SI), to be supplemented with relativistic and dynamical contributions. DFT-D3 dispersion correction[34] for potential energy was needed for the attraction between Xe and the cage when moving away from the geometric center, shown in Figure 2c. Xenon experiences shallow potential energy minima regions localized ∼1.0−1.3 Å from the geometric center of the cage toward the corners of the cavity, reflecting its structural symmetry. The low local potential maximum at the center only slightly hinders the free movement of Xe around the cage.

The reference point for the Xe chemical shift (with respect to free Xe atom) calculations was chosen to be 1.3 Å from the geometric center toward a corner Fe^{2+} ion. As displayed in Figure 2d, the nonrelativistic (NR) ^{129}Xe chemical shift at the reference point in the minimum energy region is about 100 ppm larger than at the center of the cage. Its monotonic and rapid increase toward the cage walls and, especially, corner metal ions combined with the location of the energy minima explain most of the experimentally observed large deshielding. The local potential energy maximum reduces the sampling of small chemical shift values in the center of the cage, and hence, Xe gains large chemical shift contributions when probing mainly the fringes of the cage in finite temperatures. Therefore, the cage signal exists downfield from the water signal. At the same time, the center potential maximum associated with the chemical shift minimum produces an opposite contribution to the temperature dependence compared to the wall potential, lowering the temperature derivative of the Xe shift.

The NR theory, giving the largest, +196.0 ppm, contribution to the Xe shift at the reference point, is expected to provide the overall shapes of the potential energy and NMR hypersurface. Hence, the main role of relativity is to provide the third largest additive contribution, +18.9 ppm, computed with Breit−Pauli perturbation theory (BPPT).[35] Only the five main terms (BPPT-5, see Table S3) were included that practically encompass the relativistic correction for atomistic[32] and molecular[33] Xe as well as other heavy elements.[36]

The second largest contribution to the ^{129}Xe shift comes from the Xe dynamics within the cage,[32] yielding a negative dynamical correction of −35.7 ppm at T = 300 K. It was obtained using canonical (NVT) Metropolis Monte Carlo simulations at various temperatures, where the Xe atom sampled the above-mentioned fixed potential energy and Xe shift 3D-hypersurfaces, of which 2D slices are displayed in Figure 2c,d. The Xe dynamics also explains most (0.0398 ppm/K) of the experimentally detected positive temperature derivative (0.0422 ppm/K) of ^{129}Xe shift (Table S4 and Figure S3). Relativistic Xe shift surface would probably cover most of the small residual deviation, as the relativity makes surface steeper close to the metal ion. Also the average Xe shift would be larger and, hence, closer to the experiments.

The best computational Xe NMR shift estimate (T = 300 K), +179.1 ppm, is ∼25 ppm lower than the experimental one. In addition to the missing relativistic effect on the chemical shift hypersurface discussed above, it mainly arises from the other neglected effects due to the size and complexity of the present Fe_4L_6 cage, such as cage dynamics and explicit dynamical solvent.[32,37]

In summary, the ^{129}Xe NMR experiments described in this paper prove that Fe_4L_6 metallosupramolecular cages have affinity for xenon, and the binding constant measured by ^{129}Xe NMR is 16 M^{-1}. ^{129}Xe in Fe_4L_6 has an unusual chemical shift downfield from free ^{129}Xe in water, explained by ab initio modeling to be a result of the large contributions in close contact with the cage. Also, the effects of Xe motion as well as relativistic corrections were computed to have significant contributions to the chemical shift. The slope of the linear temperature dependence of ^{129}Xe shift in cage, practically reproduced with NR motional averaging of Xe movement alone, was ∼0.042 ppm/K, and the chemical exchange rate between encapsulated and free Xe determined by 2D ^{129}Xe EXSY was 10 Hz. The results demonstrate the potential of metallosupramolecular cages in various applications, after optimizing essential properties such as cage dimensions, binding constant, and exchange rate, e.g., by changing the metals[6] or ligands.[38] The potential applications might include collecting rare gases,[20] temperature sensors based on the linear temperature dependence of the chemical shift of encapsulated Xe,[14,17] ^{129}Xe NMR-based biosensors (requiring, however, a different kind, "non-self-assembled" cage which can be functionalized),[16] and even local pH sensors.[18]

■ ASSOCIATED CONTENT

Supporting Information

Experimental and computational details. This material is available free of charge via the Internet at http://pubs.acs.org.

■ AUTHOR INFORMATION

Corresponding Authors

*ville-veikko.telkki@oulu.fi

*perttu.lantto@oulu.fi

Notes

The authors declare no competing financial interest.

■ ACKNOWLEDGMENTS

J.R. would like to acknowledge the National Doctoral Programme in Nanoscience (NGS-NANO), the Finnish Cultural Foundation and the Oulu University Scholarship Foundation for funding. P.L. (grant no. 125316) and K.R.

DOI: 10.1021/ja5130176
J. Am. Chem. Soc. 2015, 137, 2464−2467

(grant nos. 263256, 265328) thank the Academy of Finland for financial support. CSC-IT Center for Science as well as the Finnish Grid Initiative project provided the computational resources. We would like to thank Prof. Juha Vaara, Emer. Prof. Jukka Jokisaari, and Dr. Sanna Komulainen for helpful discussions.

REFERENCES

(1) (a) Lehn, J.-M. *Angew. Chem., Int. Ed. Engl.* **1988**, *27*, 89. (b) Cook, T. R.; Zheng, Y.-R.; Stang, P. J. *Chem. Rev.* **2013**, *113*, 734. (c) Chakrabarty, R.; Mukherjee, P. S.; Stang, P. J. *Chem. Rev.* **2011**, *111*, 6810. (d) Seidel, S. R.; Stang, P. J. *Acc. Chem. Res.* **2002**, *35*, 972. (e) Leininger, S.; Olenyuk, B.; Stang, P. J. *Chem. Rev.* **2000**, *100*, 853. (f) Stang, P. J.; Olenyuk, B. *Acc. Chem. Res.* **1997**, *30*, 502. (g) Yoshizawa, M.; Klosterman, J. K. *Chem. Soc. Rev.* **2014**, *43*, 1885. (h) Mitra, T.; Jelfs, K. E.; Schmidtmann, M.; Ahmed, A.; Chong, S. Y.; Adams, D. J.; Cooper, A. I. *Nat. Chem.* **2013**, *5*, 276.

(2) (a) Saha, M. L.; Schmittel, M. *Org. Biomol. Chem.* **2012**, *10*, 4651. (b) Castilla, A. M.; Ramsay, W. J.; Nitschke, J. R. *Acc. Chem. Res.* **2014**, *47*, 2063. (c) Ayme, J.-F.; Beves, J. E.; Campbell, C. J.; Leigh, D. A. *Chem. Soc. Rev.* **2013**, *42*, 1700−1712.

(3) (a) Smulders, M. M. J.; Riddell, I. A.; Browne, C.; Nitschke, J. R. *Chem. Soc. Rev.* **2013**, *42*, 1728. (b) Rotzler, J.; Mayor, M. *Chem. Soc. Rev.* **2013**, *42*, 44. (c) Acharyya, K.; Mukherjee, S.; Mukherjee, P. S. *J. Am. Chem. Soc.* **2013**, *135*, 554. (d) Samanta, S. K.; Bats, J. W.; Schmittel, M. *Chem. Commun.* **2014**, *50*, 2364.

(4) Mal, P.; Schultz, D.; Beyeh, K.; Rissanen, K.; Nitschke, J. R. *Angew. Chem., Int. Ed.* **2008**, *47*, 8297.

(5) Mal, P.; Breiner, B.; Rissanen, K.; Nitschke, J. R. *Science* **2009**, *324*, 1697.

(6) Ronson, T. K.; Giri, C.; Kodiah, B. N.; Minkkinen, A.; Topić, F.; Holstein, J. J.; Rissanen, K.; Nitschke, J. R. *Chem.—Eur. J.* **2013**, *19*, 3374.

(7) Giri, C.; Topić, F.; Mal, P.; Rissanen, K. *Dalton Trans.* **2014**, *43*, 17889.

(8) (a) Bartik, K.; Choquet, P.; Constantinesco, A.; Duhamel, G.; Fraissard, J.; Hyacinthe, J. N.; Jokisaari, J.; Locci, E.; Lowery, T. J.; Luhmer, M.; Meersmann, T.; Moudrakovski, I. L.; Pavlovskaya, G. E.; Pierce, K. L.; Pines, A.; Ripmeester, J. A.; Telkki, V.-V.; Veeman, W. S. *Actual. Chim.* **2005**, *287*, 16. (b) Goodson, B. M. *J. Magn. Reson.* **2002**, *155*, 157.

(9) (a) Albert, M. S.; Cates, G. D.; Driehuys, B.; Happer, W.; Saam, B.; Springer, C. S., Jr.; Wishnia, A. *Nature* **1994**, *370*, 199. (b) Mugler, J. P., III; Altes, T. A.; Ruset, I. C.; Dregely, I. M.; Mata, J. F.; Miller, G. W.; Ketel, S.; Ketel, J.; Hersman, F. W.; Ruppert, K. *Proc. Natl. Acad. Sci. U.S.A.* **2010**, *107*, 21707.

(10) (a) Hilty, C.; McDonnell, E. E.; Granwehr, J.; Pierce, K. L.; Han, S.; Pines, A. *Proc. Natl. Acad. Sci. U.S.A.* **2005**, *102*, 14960. (b) Telkki, V.-V.; Hilty, C.; Garcia, S.; Harel, E.; Pines, A. *J. Phys. Chem. B* **2007**, *111*, 13929.

(11) (a) Jokisaari, J. NMR of Noble Gases Dissolved in Liquid Crystals. In *NMR of Ordered Liquids*; Burnell, E. E., de Lange, C. A., Eds.; Kluwer: Dordrecht, 2003; p 109. (b) Jokisaari, J. P.; Kantola, A. M.; Lounila, J. A.; Ingman, L. P. *Phys. Rev. Lett.* **2011**, *106*, 017801.

(12) (a) Miller, J. B.; Walton, J. H.; Roland, C. M. *Macromolecules* **1993**, *26*, 5602. (b) Glöggler, S.; Raue, M.; Colell, J.; Türschmann, P.; Liebisch, A.; Mang, T.; Blümich, B.; Appelt, S. *ChemPhysChem* **2012**, *13*, 4120.

(13) (a) Demarquay, J.; Fraissard, J. *Chem. Phys. Lett.* **1987**, *136*, 314. (b) Terskikh, V. V.; Moudrakovski, I. L.; Breeze, S. R.; Lang, S.; Ratcliffe, C. I.; Ripmeester, J. A.; Sayari, A. *Langmuir* **2002**, *18*, 5653. (c) Telkki, V.-V.; Lounila, J.; Jokisaari, J. *J. Chem. Phys.* **2006**, *124*, 034711.

(14) Saunavaara, J.; Jokisaari, J. J. *J. Magn. Reson.* **2006**, *180*, 58.

(15) (a) Spence, M. M.; Rubin, S. M.; Dimitrov, I. E.; Ruiz, E. J.; Wemmer, D. E.; Pines, A.; Yao, S. Q.; Tian, F.; Schultz, P. G. *Proc. Natl. Acad. Sci. U.S.A.* **2001**, *98*, 10654. (b) Schröder, L.; Lowery, T. J.; Hilty, C.; Wemmer, D. E.; Pines, A. *Science* **2006**, *314*, 446. (c) Huber, G.; Brotin, T.; Dubois, L.; Desvaux, H.; Dutasta, J.-P.; Berthault, P. *J. Am. Chem. Soc.* **2006**, *128*, 6239. (d) Seward, G. K.; Bai, Y.; Khan, N. S.; Dmochowski, I. J. *Chem. Sci.* **2011**, *2*, 1103. (e) Rosea, H. M.; Wittea, C.; Rossella, F.; Klippel, S.; Freund, C.; Schröder, L. *Proc. Natl. Acad. Sci. U.S.A.* **2014**, *111*, 11697.

(16) Schröder, L. *Phys. Med.* **2013**, *29*, 3.

(17) (a) Schilling, F.; Schröder, L.; Palaniappan, K. K.; Zapf, S.; Wemmer, D. E.; Pines, A. *ChemPhysChem* **2010**, *11*, 3529. (b) Huber, G.; Beguin, L.; Desvaux, H.; Brotin, T.; Fogarty, H. A.; Dutasta, J.-P.; Berthault, P. *J. Phys. Chem. A* **2008**, *112*, 11363.

(18) Berthault, P.; Desvaux, H.; Wendlinger, T.; Gyejacquot, M.; Stopin, A.; Brotin, T.; Dutasta, J.-P.; Boulard, Y. *Chem.—Eur. J.* **2010**, *16*, 12941.

(19) Riddell, I. A.; Smulders, M. M. J.; Clegg, J. K.; Nitschke, J. R. *Chem. Commun.* **2011**, *47*, 457.

(20) Chen, L.; Reiss, P. S.; Chong, S. Y.; Holden, D.; Jelfs, K. E.; Hasell, T.; Little, M. A.; Kewley, A.; Briggs, M. E.; Stephenson, A.; Thomas, K. M.; Armstrong, J. A.; Bell, J.; Busto, J.; Noel, R.; Liu, J.; Strachan, D. M.; Thallapally, P. K.; Cooper, A. I. *Nat. Mater.* **2014**, *13*, 954.

(21) Kennan, R. P.; Pollack, G. L. *J. Chem. Phys.* **1990**, *93*, 2724.

(22) Amor, N.; Zänker, P. P.; Blümler, P.; Meise, F. M.; Schreiber, L. M.; Scholz, A.; Schmiedeskamp, J.; Spiess, H. W.; Münnemann, K. *J. Magn. Reson.* **2009**, *201*, 93.

(23) Fairchild, R. M.; Joseph, A. I.; Holman, K. T.; Fogarty, H. A.; Brotin, T.; Dutasta, J.-P.; Boutin, C.; Huber, G.; Berthault, P. *J. Am. Chem. Soc.* **2010**, *132*, 15505.

(24) Bagno, A.; Saielli, G. *Chem.—Eur. J.* **2012**, *18*, 7341.

(25) Jeener, J.; Meier, B. H.; Bachmann, P.; Ernst, R. R. *J. Chem. Phys.* **1979**, *71*, 4546.

(26) Abragam, A. *The Principles of Nuclear Magnetism*; Clarendon: Oxford, 1974.

(27) Ylihautala, M.; Lounila, J.; Jokisaari, J. J. *Chem. Phys.* **1999**, *110*, 6381.

(28) *TURBOMOLE*, V6.5; TURBOMOLE GmbH: Karlsruhe, Germany, 2013; http://www.turbomole.com.

(29) *DALTON 2013.4*, 2014; http://daltonprogram.org.

(30) (a) Schäfer, A.; Horn, H.; Ahlrichs, R. *J. Chem. Phys.* **1992**, *97*, 2571. (b) Weigend, F.; Ahlrichs, R. *Phys. Chem. Chem. Phys.* **2005**, *7*, 3297.

(31) (a) Lee, C.; Yang, W.; Parr, R. G. *Phys. Rev. B* **1988**, *37*, 785. (b) Becke, A. D. *J. Chem. Phys.* **1993**, *98*, 1372.

(32) Straka, M.; Lantto, P.; Vaara, J. *J. Phys. Chem. A* **2008**, *112*, 2658.

(33) (a) Lantto, P.; Vaara, J. *J. Chem. Phys.* **2007**, *127*, 084312. (b) Straka, M.; Lantto, P.; Vaara, J. *J. Chem. Phys.* **2007**, *127*, 234314. (c) Lantto, P.; Standara, S.; Riedel, S.; Vaara, J.; Straka, M. *Phys. Chem. Chem. Phys.* **2012**, *14*, 10944.

(34) Grimme, S.; Anthony, J.; Ehrlich, S.; Krieg, H. *J. Chem. Phys.* **2010**, *132*, 154104.

(35) (a) Manninen, P.; Lantto, P.; Vaara, J.; Ruud, K. *J. Chem. Phys.* **2003**, *119*, 2623. (b) Manninen, P.; Ruud, K.; Lantto, P.; Vaara, J. *J. Chem. Phys.* **2005**, *122*, 114107. (c) Manninen, P.; Ruud, K.; Lantto, P.; Vaara, J. *J. Chem. Phys.* **2006**, *124*, 149901(E). (d) Vaara, J.; Manninen, P.; Lantto, P. In *Calculation of NMR and EPR Parameters: Theory and Applications*; Kaupp, M., Bühl, M., Malkin, V. G., Eds.; Wiley-VCH: Weinheim, Germany, 2004; pp 209−226.

(36) Roukala, J.; Maldonado, A. F.; Vaara, J.; Aucar, G. A.; Lantto, P. *Phys. Chem. Chem. Phys.* **2011**, *13*, 21016.

(37) (a) Standara, S.; Kulhánek, P.; Marek, R.; Horníček, J.; Bouř, P.; Straka, M. *Theor. Chem. Acc.* **2011**, *129*, 677. (b) Standara, S.; Kulhánek, P.; Marek, R.; Straka, M. *J. Comput. Chem.* **2013**, *34*, 1890.

(38) Meng, W.; Ronson, T. K.; Nitschke, J. R. *Proc. Natl. Acad. Sci. U.S.A.* **2013**, *110*, 10531.

DOI: 10.1021/ja5130176
J. Am. Chem. Soc. 2015, 137, 2464−2467